Chinese Journal of Physics 89 (2024) 493–503

Contents lists available at ScienceDirect

Chinese Journal of Physics

journal homepage: www.elsevier.com/locate/cjph

Maximizing heat transfer and minimizing entropy generation in concentric cylinders with CuO–MgO–TiO_2 nanoparticles

Hanifa Hanif [a,b,*], Sharidan Shafie [b], Zainab Toyin Jagun [c,*]

[a] Department of Mathematics, Sardar Bahadur Khan Women's University, Quetta, Pakistan
[b] Department of Mathematical Sciences, Faculty of Science, Universiti Teknologi Malaysia, 81310 Johor Bahru, Johor, Malaysia
[c] Department of Real Estate, School of Built Environment, Engineering & Computing, Leeds Beckett University, NT212, Northern Terrace, City Campus, Leeds LS2 8AG, United Kingdom

ARTICLE INFO

Keywords:
Entropy generation
Ternary nanofluid
Nanoparticles
Cylindrical flow

ABSTRACT

Heat transfer is crucial because it has industrial uses. A novel type of nanofluids dubbed "ternary nanofluid" is being utilized to boost the ability of conventional fluids to transmit heat since it has a greater heat transfer capacity than solo and hybrid nanofluids. This work investigates the heat transfer capabilities and entropy generation in the cylindrical flow of a ternary nanofluid in the presence of a magnetic field. Minimizing the entropy generation and maximizing the heat transfer of a fluid using ternary nanoparticles (CuO–MgO–TiO_2) is the aim of this work. The finite difference method is used by the MATLAB computer program to solve the problem numerically. The results reveal that the entropy generation minimizes in the presence of CuO–MgO–TiO_2. The heat transfer rate of the fluid increased by 9.9%, 10.8%, and 11.2% on adding TiO_2, MgO–TiO_2, and CuO–MgO–TiO_2 nanoparticles, respectively.

1. Introduction

One of the most significant and essential natural processes at the industrial level is the flow and heat transfer process through a cylindrical structure. It may be used in many different industrial manufacturing processes, including metal spinning, cancer therapy, optical fiber coating, and the synthesis of nanowires. The primary question is why we employ cylindrical forms for all of these processes so frequently. There are numerous facts to consider, but the most essential is to lower the drag force with the surface so that the fluid may flow quicker in cylindrical form than in other shapes. Researchers are interested in the consequences of flow and heat transfer through cylinders, for instance, Shaikh et al. [1] investigated the hydrodynamic properties of continuous rectilinear torsional flow of pseudoplastic fluid between two coaxial cylinders and observed that when the outer cylinder spins while the inner cylinder remains at rest, fluid lags near the inner cylinder for small radius ratios and velocity appears linear for large radius ratios. Regarding cooling applications, Laidoudi and Ameur [2] analyzed the convection heat transfer of fluid between concentric cylinders. Gouran et al. [3] investigated the impact of radiation on the magnetohydrodynamic fluid flow between two circular cylinders. Abro and Abdon [4] analyzed the dynamics of fractional Oldroyd-B fluid between concentric cylinders. Their results indicate that smaller values of thermal relaxation time cause oscillation between temperature distribution and Prandtl number causing thermal fluctuations with inherent structure. Zhang et al. [5] investigated the behavior of viscoelastic fluid flow between concentric cylinders, and claimed that raising the exponent parameter causes the temperature to rise close to the inner cylinder but to drop close to the external cylinder, indicating that doing so can improve heat transmission.

* Corresponding authors.
E-mail addresses: hanifahanif@outlook.com (H. Hanif), z.t.jagun@leedsbeckett.ac.uk (Z.T. Jagun).

https://doi.org/10.1016/j.cjph.2023.12.021
Received 27 September 2023; Received in revised form 30 November 2023; Accepted 13 December 2023
Available online 27 December 2023
0577-9073/

Recent advances in nanotechnology have disclosed a brand-new source of energy by using nanofluids, which are created by the dispersion of nano-sized particles in conventional fluids. This approach identifies different features of the extraordinary increase in thermal efficiency of heat exchangers, solar sectors, power manufacturing, and energy storage systems [6–8]. Following Choi and Eastman [9] initial work, in which nanoparticles dissolved in water-based fluid were used to illustrate the dominant thermal properties of nanofluid, multiple studies have been done with different versions with broader applicability [10–12]. Nanoparticles can be metal, metal-oxide, and carbonized. The distinct features of manmade metal-oxide nanoparticles have made them one of the most widely utilized produced nanomaterials [13]. Due to their numerous industrial, medicinal, and military uses, metal oxide nanoparticles, such as copper oxide (CuO), magnesium oxide (MgO), and titanium dioxide (TiO_2), have drawn more attention [14–17]. The possible environmental and industrial use of these metal oxide nanoparticles has been studied in light of their widespread applications. Naveena et al. [18] scrutinized the properties of La-doped and CuO thin films and found that La-dopped CuO thin films may be utilized as an effective absorber material for a solar cell. Rymar [19] studied the hydrodynamics of TiO_2/water nanofluid in a slinky collector of the heat pump and noticed that the performance efficiency coefficient of TiO_2/water was 1.118 and 1.091 during the heating and non-heating seasons, respectively. Kho et al. [20] claimed that TiO_2 nanoparticles are capable of reducing the skin friction coefficients and increasing the thermal conductivity of the fluid. Tuncer et al. [21] used TiO_2 and hybrid composite TiO_2–CuO to improve the thermal performance of newly developed shell and helically coiled heat exchangers. They noticed that adding TiO_2 and TiO_2–CuO in the base fluid water significantly intensified the overall heat transfer coefficient up to 8.6% and 12%, respectively. Azmi et al. [22] discussed the mechanical Performance of intumescent coating and claimed that the thermal performance of coating might be improved with MgO nanoparticles. Aytaç et al. [23] presented an experimental analysis of the impacts of using MgO–CuO/water nanofluid on the thermal performances of a heat pipe evacuated solar water collector. Their experimental results indicate that the system's thermal efficiencies with water ranged from 49.62% to 56.18% whereas using MgO–CuO/water as the working fluid it ranged from 69.89% to 77.21%. Tlili et al. [24] claimed that CuO–MgO/methanol hybrid nanofluid may be used as an insulator on comparing its properties to CuO/methanol nanofluid.

An advanced class of nanofluid technology has been introduced as a ternary nanofluid, which is a mixture of three distinct types of nanoparticles and a base fluid. Ternary nanofluid is capable of transferring more heat compared to nanofluid and hybrid nanofluids. In general, both nanofluids and hybrid nanofluids have shown great promise as heat transfer fluids, the development of ternary nanofluids provides additional benefits that can make them even more effective in various industrial and engineering applications. As a result, research has been done on the thermal and physical features of ternary nanofluids, some of which are given here. Because of its large heat capacity, water can absorb and hold a lot of heat without experiencing a noticeable temperature change. The dynamics of a water-based ternary-hybrid nanofluid of different water temperatures on a wedge were studied in [25–28]. It was discovered that heat transfer is slow at first since few nanoparticles are present. The findings of an investigation by Mousavi et al. [29] into the significances of temperature, volume concentration of nanoparticles on the thermo-physical characteristics of the CuO–MgO–TiO_2/Water ternary nanofluid demonstrate that the nanoparticle ratio is crucial for the thermal enhancement. The Al_2O_3–CuO–TiO_2/water ternary nanofluid's response to temperature and volume fraction was investigated by Sahoo and Kumar [30]. The 0.1 vol% ternary nanofluid showed increases in viscosity of 17.25% and 55.41% when compared to CuO–Al_2O_3/water and TiO_2–Al_2O_3/water. Boroomandpour et al. developed a novel correlation to predict the thermal conductivity of the MWCNTs-TiO_2–ZnO/water-ethylene glycol ternary nanofluid as a function of nanoparticle fraction and temperature based on experimental results [31]. The stability and thermal conductivity of rGO–Fe_3O_4–TiO_2/ethylene glycol ternary nanofluid were studied by Cakmak et al. [32], who discovered that the rise in thermal conductivity increased dramatically with temperature and mass concentration. Experimental research was done on the thermo-economic behavior of the water–based Al_2O_3–TiO_2–Cu ternary nanofluid by Xuan et al. [33]. According to the findings, the ideal mixture ratio 40(Al_2O_3):40(TiO_2):20(Cu) had the minimum viscosity and maximum thermal conductivity. Furthermore, the most effective working fluids in the turbulent and laminar flow regimes, respectively, were ternary nanofluids with 1 vol% and 0.7 vol%.

The minimizing of entropy generation has been accomplished in recent years by using thermodynamics second law to identify the best engineering systems. The amount of irreversibilities that build up throughout a process is determined by the production of entropy. Entropy production may therefore be used as a metric to evaluate the effectiveness of engineering equipment [34]. According to Mondal and Mahapatra [35], a low magnetic field is more suitable to minimize the overall entropy generation in a rectangular cavity. Additionally, It has been claimed that entropy generation is mostly influenced by heat transport and that entropy generation is decreased by Richardson numbers with lower values (Ri = 0.01). Hanif et al. [36] discussed the heat transfer and entropy generation in magnetized nanofluid. Manna et al. [37] studied heat transfer and entropy generation in cavities using a hybrid nanofluid in the presence of a magnetic field. According to their results, the mechanism of heat transport is greatly regulated by the Lorentz force, and the heating-cooling junction point is where the highest entropy generation is found. Sahoo [38] has looked at a ternary nanofluid with three different shaped nanoparticles, including aluminum oxide (spherical), carbon nanotubes (cylindrical), and graphene (platelet), as a novel radiator coolant. A shift in ternary hybrid concentrations between 1% and 3%, however, results in a 42.45% increase in irreversibility. The effects of magnetic field on entropy generation in Eyring–Powell fluid in the presence of Au–Ag hybrid nanoparticle is studied by Bhatti et al. [39]. They found that entropy generation increased for increasing estimates of magnetic parameter, nanoparticles volume fraction. Mallick and Misra [40] investigated entropy production in electrically regulated transit of a nanofluid in a hydrophobic cylindrical microtube. Based on their investigation, the system's total entropy is discovered to be lowered due to nonlinear radiation, suggesting improved system performance. Fares et al. [41] presented an optimal entropy generation in the magnetized flow of Ag/water nanofluid in a porous cavity, and observed that entropy development decreases due to the magnetic field.

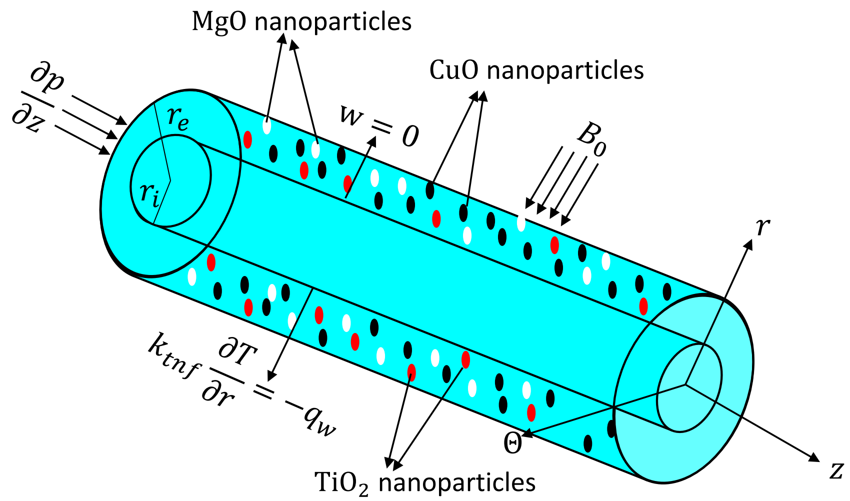

Fig. 1. Graphical representation.

Table 1
Thermo-physical properties of water and nanoparticles [20,24].

Materials	ρ kgm^{-3}	σ Sm^{-1}	C_p J (kgK)$^{-1}$	k W (mK)$^{-1}$
Water	997.1	0.05	4179	0.613
CuO	6320	6.9×10^{-2}	531.8	76.5
MgO	3580	1.42×10^{-3}	960	48.4
TiO_2	4250	2.6×10^{6}	686.2	8.9538

The above literature reveals that a number of studies discussed the fluid flow between two concentric cylinders, however, no research has been made to discuss the behavior of fluid in the presence of ternary nanoparticles. This research attempts to fill this gap by exploring the effects of CuO–MgO–TiO_2 on the thermal performance of a water-based fluid flow between two concentric cylinders. Moreover, entropy generation minimization is essential because it is a way of thermodynamic optimization of real-world devices and processes. We may limit the irreversibilities and losses that occur in any practical process by minimizing entropy creation, and so enhance the usable work output or lower the input energy need. Therefore, the ultimate goal of this study is to analyze heat transfer and entropy generation in a fluid flow between two concentric cylinders due to ternary nanoparticles. Such a contribution would be helpful for controlling energy consumption, enhancing thermal efficiency, and optimizing the irreversibilities—all of which are significant issues facing the industry. This research seeks to determine the responses to the following questions:

- What are the consequences of ternary nanoparticles on the dynamics of fluid flow between concentric cylinders?
- How do ternary nanocomposites behave when a magnetic field is employed normal to the flow direction?
- How to maximize the heat transfer rate and minimize the entropy generation in a thermal system?

2. Problem description

Mainstream flow is generated by an applied pressure gradient

$$\frac{1}{\rho_f}\frac{\partial p}{\partial z} = -a_0 H(t), \tag{1}$$

where ρ_f is the density of the fluid, a_0 is the constant pressure gradient coefficient, and H is unit step function defined as:

$$H(t) = \begin{cases} 0 & t < 0, \\ 1 & t > 0. \end{cases} \tag{2}$$

2.1. Assumptions

The following assumptions and conditions are noted for the mathematical simulation:

- Laminar, two-dimensional, and time-dependent cylindrical flow
- Single phase nanofluid

Table 2
Thermo-physical properties of nanofluid, hybrid nanofluid, and ternary nanofluid [42,43].

Properties	Mathematical expressions
Viscosity	$\mu_{nf}=\dfrac{\mu_f}{(1-\phi_1)^{2.5}},\quad \mu_{hnf}=\dfrac{\mu_{nf}}{(1-\phi_2)^{2.5}},\quad \mu_{tnf}=\dfrac{\mu_{hnf}}{(1-\phi_3)^{2.5}}$
Density	$\rho_{nf}=(1-\phi_1)\rho_f+\phi_1\rho_{n_1},\quad \rho_{hnf}=(1-\phi_2)\rho_{nf}+\phi_2\rho_{n_2},$ $\rho_{tnf}=(1-\phi_3)\rho_{hnf}+\phi_3\rho_{n_3}$
Heat capacity	$(\rho C_p)_{nf}=(1-\phi_1)(\rho C_p)_f+\phi_1(\rho C_p)_{n_1},\quad (\rho C_p)_{hnf}=(1-\phi_2)(\rho C_p)_{nf}$ $+\phi_2(\rho C_p)_{n_2},\quad (\rho C_p)_{tnf}=(1-\phi_3)(\rho C_p)_{hnf}+\phi_3(\rho C_p)_{n_3}$
Electrical conductivity	$\dfrac{\sigma_{nf}}{\sigma_f}=\dfrac{\sigma_{n_1}+2\sigma_f+2\phi_1(\sigma_{n_1}-\sigma_f)}{\sigma_{n_1}+2\sigma_f-\phi_1(\sigma_{n_1}-\sigma_f)},\quad \dfrac{\sigma_{hnf}}{\sigma_{nf}}=\dfrac{\sigma_{n_2}+2\sigma_{nf}+2\phi_2(\sigma_{n_2}-\sigma_{nf})}{\sigma_{n_2}+2\sigma_{nf}-\phi_2(\sigma_{n_2}-\sigma_{nf})},$ $\dfrac{\sigma_{tnf}}{\sigma_{hnf}}=\dfrac{\sigma_{n_3}+2\sigma_{hnf}+2\phi_3(\sigma_{n_3}-\sigma_{hnf})}{\sigma_{n_3}+2\sigma_{hnf}-\phi_3(\sigma_{n_3}-\sigma_{hnf})}$
Thermal conductivity	$\dfrac{k_{nf}}{k_f}=\dfrac{k_{n_1}+2k_f+2\phi_1(k_{n_1}-k_f)}{k_{n_1}+2k_f-\phi_1(k_{n_1}-k_f)},\quad \dfrac{k_{hnf}}{k_{nf}}=\dfrac{k_{n_2}+2k_{nf}+2\phi_2(k_{n_2}-k_{nf})}{k_{n_2}+2k_{nf}-\phi_2(k_{n_2}-k_{nf})},$ $\dfrac{k_{tnf}}{k_{hnf}}=\dfrac{k_{n_3}+2k_{hnf}+2\phi_3(k_{n_3}-k_{hnf})}{k_{n_3}+2k_{hnf}-\phi_3(k_{n_3}-k_{hnf})}$

- CuO, MgO, and TiO_2 nanoparticles
- Water as a base fluid
- Two concentric cylinders
- Pressure gradient in z–direction
- Magnetic field normal to the flow direction
- Heat flux conditions $k_{tnf}\dfrac{\partial T}{\partial r}=-q_w$ at the inner cylinder

The graphical model is presented in Fig. 1. The thermo-physical properties of the CuO, MgO, TiO_2, and water are listed in Table 1. The mathematical expressions for the properties of nanofluid, hybrid nanofluid, and ternary nanofluid are depicted in Table 2.

2.2. Mathematical formulation

The governing equations for the heat transfer and unsteady flow of a ternary nanofluid in the presence of magnetic field are:

$$\rho_{tnf}\frac{\partial w}{\partial t}=-\frac{\partial p}{\partial z}+\mu_{tnf}\left(\frac{\partial^2 w}{\partial r^2}+\frac{1}{r}\frac{\partial w}{\partial r}\right)-\sigma_{tnf}B_0^2 w. \tag{3}$$

$$(\rho C_p)_{tnf}\left(\frac{\partial T}{\partial t}+w\frac{\partial T}{\partial z}\right)=k_{tnf}\left(\frac{\partial^2 T}{\partial r^2}+\frac{1}{r}\frac{\partial T}{\partial r}+\frac{\partial^2 T}{\partial z^2}\right). \tag{4}$$

The imposed initial and boundary conditions are

$$\begin{aligned} &w(r,z,0)=0,\quad w(r_i,z,T)=0,\quad w(r_e,z,T)=0,\\ &T(r,z,0)=0,\quad k_{tnf}\frac{\partial T}{\partial r}(r_i,z,T)=-q_w,\quad \frac{\partial T}{\partial r}(r_e,z,T)=0. \end{aligned} \tag{5}$$

It is worth mentioning that the fluid is allowed to flow within two concentric cylinders with the velocity $V=(0,0,w(r,t,z))$.

2.3. Non-dimensional flow model

We introduce a set of non-dimensional parameters which help us in obtaining the non-dimensional form of the considered model:

$$r^*=\frac{r}{r_e},\ z^*=\frac{z}{r_e},\ t^*=\frac{t\nu_f}{r_e^2}\ w^*=\frac{wr_e}{\nu_f},\ T^*=\frac{T-T_f}{\Delta T},\ \Delta T=\frac{q_w r_e}{k_f}. \tag{6}$$

Using Eq. (6) in Eqs. (3)–(5), we have

$$\zeta_1\frac{\partial w}{\partial t}=p_0 H(t)+\zeta_2\left(\frac{\partial^2 w}{\partial r^2}+\frac{1}{r}\frac{\partial w}{\partial r}\right)-\zeta_3 M w. \tag{7}$$

$$\zeta_4\left(\frac{\partial T}{\partial t}+w\frac{\partial T}{\partial z}\right)=\frac{\zeta_5}{Pr}\left(\frac{\partial^2 T}{\partial r^2}+\frac{1}{r}\frac{\partial T}{\partial r}+\frac{\partial^2 T}{\partial z^2}\right). \tag{8}$$

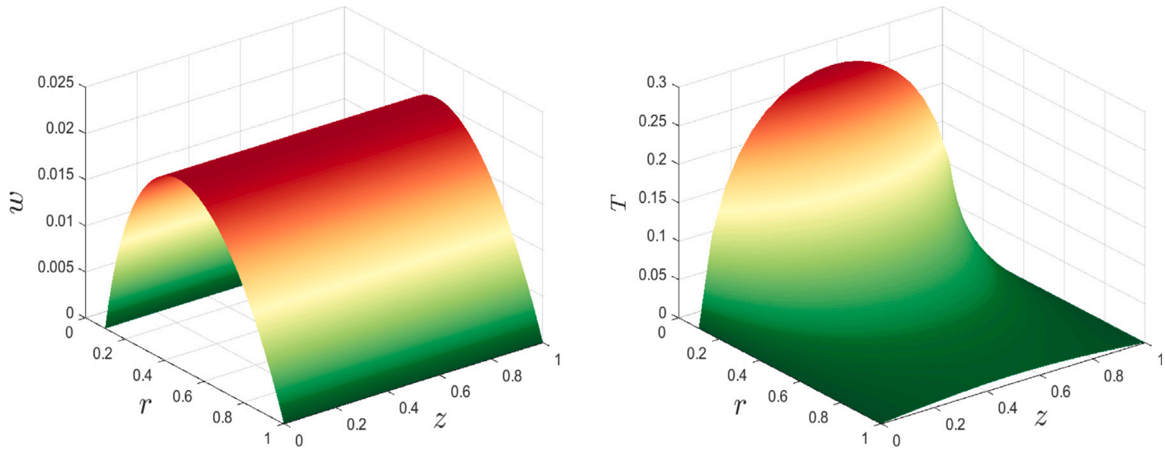

Fig. 2. Surface plots: Velocity (left); Temperature (right).

The corresponding initial and boundary conditions are

$$w(r,z,0)=0, w(R,z,t)=0, w(1,z,T)=0,$$
$$T(r,z,0)=0, \zeta_5\frac{\partial T}{\partial r}(R,z,T)=-1, \frac{\partial T}{\partial r}(1,z,T)=0. \tag{9}$$

The non-dimensional parameters p_0, M, Pr and the nanofluid constants $\zeta_1-\zeta_5$ are listed below

$$p_0=\frac{a_0r_e^3}{v_f^2},\ M=\frac{\sigma_fB_0^2r_e^2}{\mu_f},\ Pr=\frac{(\mu C_p)_f}{k_f},\ \zeta_1=(1-\phi_3)\frac{\rho_{hnf}}{\rho_f}+\phi_3\frac{\rho_{n_3}}{\rho_f},$$
$$\zeta_2=\frac{\mu_{hnf}}{\mu_f(1-\phi_3)^{2.5}},\ \zeta_3=\frac{\sigma_{tnf}}{\sigma_f},\ \zeta_4=(1-\phi_3)\frac{(\rho C_p)_{hnf}}{(\rho C_p)_f}+\phi_3\frac{(\rho C_p)_{n_3}}{(\rho C_p)_f},\ \zeta_5=\frac{k_{tnf}}{k_f}. \tag{10}$$

The Nusselt number (Nu) is defined as $Nu=r_eq_w/k_f(T_i-T_f)$. Using Eq. (6), we have$Nu=1/T(R)$.

3. Entropy analysis

Let χ_1 and χ_2 be the irreversibility due to heat transfer and fluid friction, respectively, and defined as

$$\chi_1=\frac{k_{tnf}}{T_f^2}\left[\left(\frac{\partial T}{\partial r}\right)^2+\left(\frac{\partial T}{\partial z}\right)^2\right],$$
$$\chi_2=\frac{1}{T_f}\left[\mu_{hnf}\left(\frac{\partial w}{\partial r}\right)^2+\sigma_{hnf}B_0^2w^2\right]. \tag{11}$$

Note that the total entropy generation in a system is

$$\chi_{gen}=\chi_1+\chi_2. \tag{12}$$

Using Eqs. (6), (11) and (12), we arrived at

$$S_{gen}=\frac{\chi_{gen}}{S_0}=\zeta_5\left[\left(\frac{\partial T}{\partial r}\right)^2+\left(\frac{\partial T}{\partial z}\right)^2\right]+\frac{Br}{\Omega}\left[\zeta_2\left(\frac{\partial w}{\partial r}\right)^2+\zeta_3Mw^2\right], \tag{13}$$

given that

$$S_0=\frac{k_f\Delta T}{T_f^2r_e^2},\ Br=\frac{\mu_fv_f^2}{k_f\Delta Tr_e^2},\ \Omega=\frac{T_f}{\Delta T}. \tag{14}$$

The ratio of entropy creation owing to heat transfer to overall entropy production is known as Bejan number, defined as

$$Be=\frac{\chi_1}{\chi_1+\chi_2}. \tag{15}$$

The Bejan number has a value between 0 and 1. $Be=0$ implies that χ_1 has been beaten by χ_2, but $Be=1$ shows that χ_1 has conquered χ_2. The Be value is 0.5 if the entropy created by fluid friction and heat transport contribute equally.

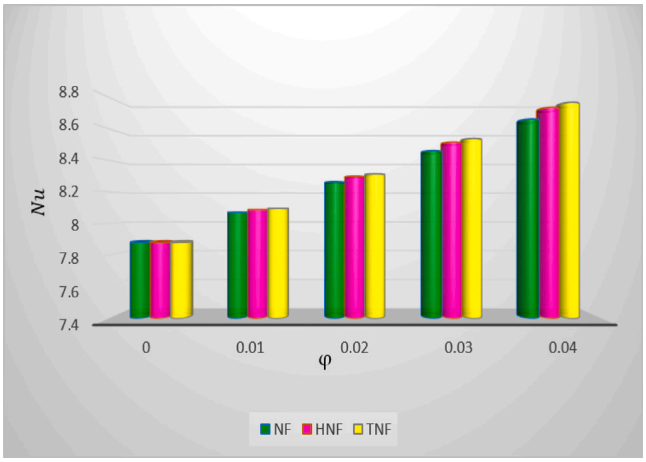

Fig. 3. Nusselt number against φ for different fluids.

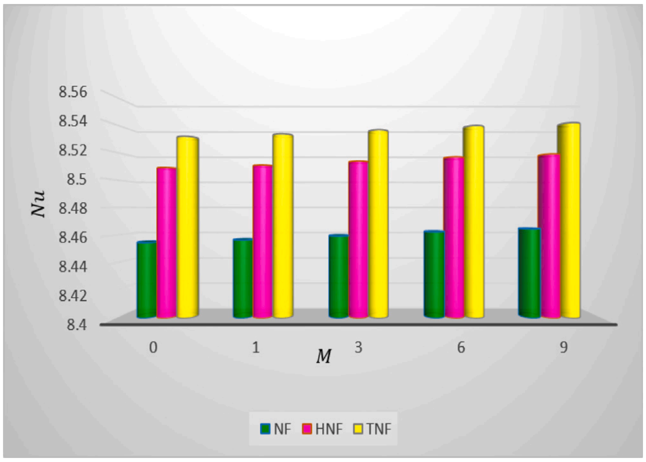

Fig. 4. Nusselt number against M for different fluids.

4. Results and discussion

The non-dimensional partial differential equations Eqs. (7) and (8) as well as the entropy generation Eq. (13) are solved using an implicit finite difference method [44–46]. The numerical results of the velocity, temperature, Nusselt number, entropy, and Bejan number are presented graphically in Figs. 2–10. The fixed values assigned to controlling variables are $\varphi = 0.03, M = 3, p_0 = 0.5, Br = 0.4$ and $\Omega = 0.3$. Surface plots for velocity and temperature are plotted in Fig. 2. The heat transfer rates of different fluids, namely, nanofluid, hybrid nanofluid, and ternary nanofluid have been compared for different values of φ and M in Figs. 3 and 4, respectively. Herein NF, HNF, and TNF refer to TiO_2/water, MgO–TiO_2/water, and CuO–MgO–TiO_2/water, respectively. Nusselt number and volume concentration for solo, hybrid, and ternary nanoparticles showed a substantial association in Fig. 3. The higher volume concentration of nanoparticles causes an immediate rise in heat transfer rates. Additionally, the heat transfer rates of ternary nanofluid are considerably greater compared to nanofluid and hybrid nanofluid. Furthermore, the heat transfer rate of the fluid increased by 9.9%, 10.8%, and 11.2% on adding TiO_2, MgO–TiO_2, and CuO–MgO–TiO_2 nanocomposites, respectively. The effects of magnetic parameter M on the Nusselt number of three different fluids are illustrated in Fig. 4. The results showed that the Nusselt number increases when M increases for all types of fluid. Due to the considerable enhancement in heat conductivity by CuO–MgO–TiO_2 nanoparticles, ternary nanofluid has the highest heat transfer rates. The frequency of convectional heat transfer is dependent on thermal conductivity, which is the cause of this behavior.

The changes in fluid velocity due to nanomaterial size φ are depicted in Fig. 5. The velocity drops as the nanoparticle volume fraction grows. It is important to mention that the viscosity and density of the ternary nanofluid are affected by the volume fraction, shape, and size of the nanoparticles. The greater the volume percentage of the nanoparticles, the more they interact with one another and with the base fluid, causing increased flow resistance and decreased velocity. Fig. 6 illustrates how the magnetic parameter M affects the velocity profile of ternary nanofluids. The velocity of nanofluids decreases as the projected value of M rises. The Lorentz

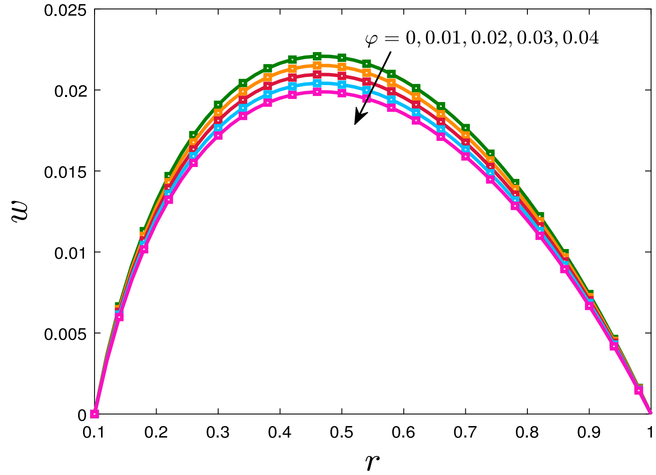

Fig. 5. Impact of nanoparticle volume fraction φ on velocity.

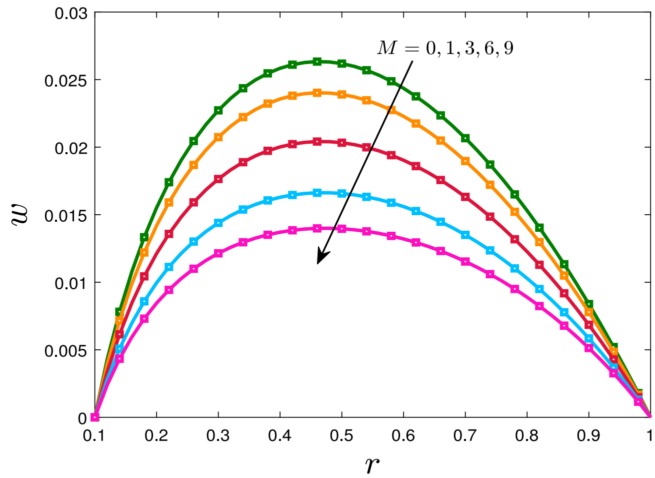

Fig. 6. Impact of magnetic parameter M on velocity.

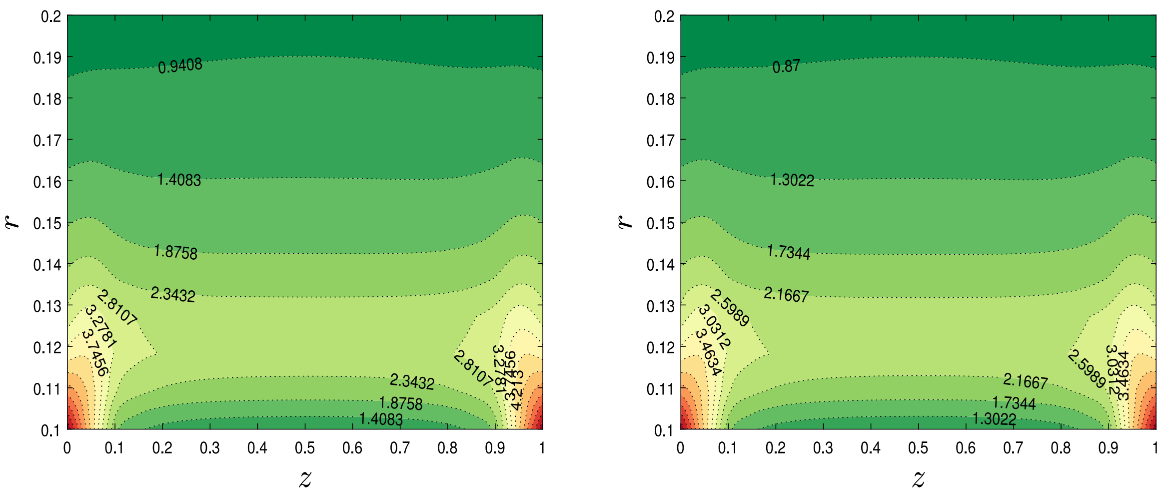

(a) Water (b) Ternary nanofluid

Fig. 7. Entropy generation of water and ternary nanofluid.

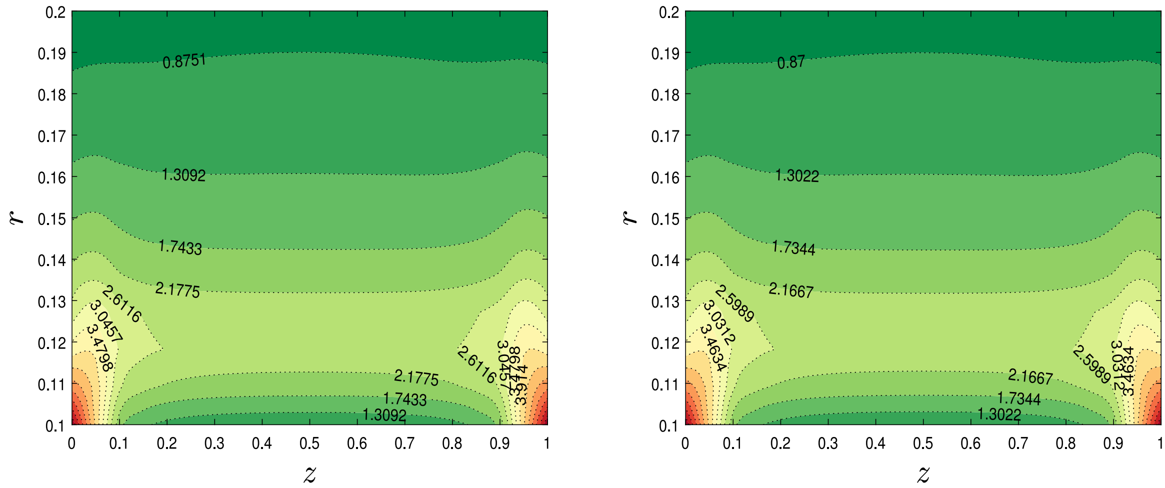

(a) $M = 0$ (b) $M = 3$

Fig. 8. Impact of magnetic parameter M on entropy generation.

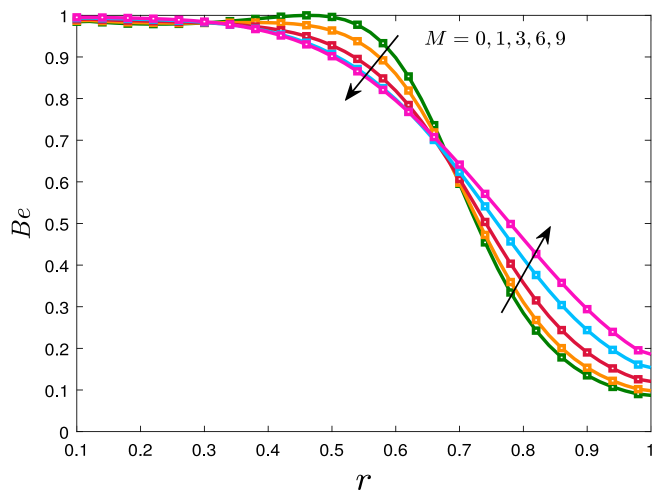

Fig. 9. Impact of magnetic parameter M on Bejan number.

force, which operates on the fluid as a result of the interaction of the magnetic field and the electric current in the fluid, causes the fluid's velocity to drop as the magnetic parameter rises. In other words, the Lorentz force opposes fluid motion and generates a drag force, lowering fluid velocity. The 2D contour plots for entropy generation in water and ternary nanofluid are depicted in Fig. 7. The results indicate that the entropy generation is higher near the inner cylinder. It can also be noticed that the entropy generation minimizes when ternary nanofluid is used instead of the base fluid water. This indicates that minimization of entropy generation may be possible using nanoparticles. It is worth mentioning that entropy generation is a measure of the irreversibilities or inefficiencies of a process. The losses and irreversibilities that occur in a process might be reduced by minimizing entropy formation, increasing useful work output, or decreasing input energy consumption. Several factors influence entropy generation, therefore, Fig. 8 has been illustrated to know the impact of a magnetic field on entropy generation of ternary nanofluid. It is evident that when the magnetic field is applied the entropy generation minimizes which is the ultimate goal of the current study.

The Bejan number is useful for determining the irreversibility distribution. It is a ratio of heat transfer entropy generation to total entropy generation. The variations in Bejan number due to the applied magnetic field are determined and illustrated in Fig. 9. Bejan number showed a dual nature against magnetic parameter M, it increased in regime close to the external cylinder for higher values of M while dropping down in the middle of the cylinders. The Bejan number reduces in the middle of the cylinder which indicates that the entropy generation due to heat transfer decreases when the magnetic field is applied and grows eventually. On the other hand, an increament in the Bejan number colse to the external cylinder is an indication of a reduction in the total entropy generation due to increasing estimates of the magnetic parameter. The effects of the magnetic field near the inner cylinder are negligible. The

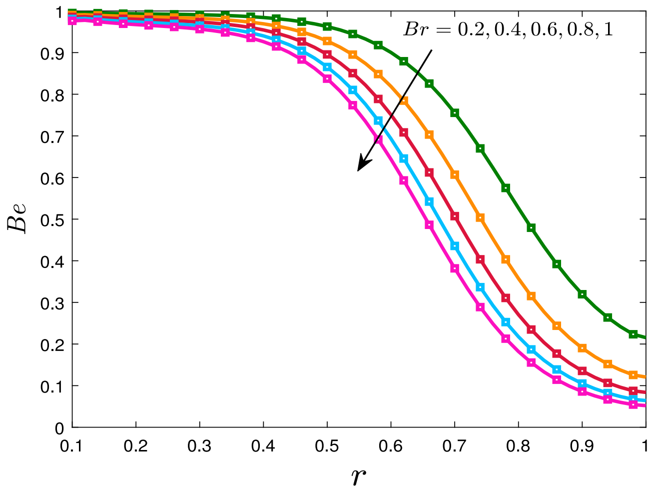

Fig. 10. Impact of Brinkman number Br Bejan number.

consequences of the Brinkman number on the Bejan number are illustrated in Fig. 10. The Brinkman number quantifies the relevance of viscous heating in comparison to conductive heat transfer. It is evident that the Bejan number decreases when Brinkman number increases showing that the Brinkman number significantly affects the entropy generation, however, the effects are negligible in the flow regime close to the inner cylinder. It is also noted that the total entropy generation is defeated by the entropy generation due to heat transfer when $r \leq 0.5$ and dominated near the external cylinder.

5. Conclusions

The goal of the current study is to examine the heat transmission together with entropy generation in a ternary fluid flow between two concentric cylinders. The flow is influenced by pressure gradient and magnetic field. The key findings of the research are:

- With the high concentration of the nanoparticles, the fluid becomes more viscous and results in a reduced velocity.
- The heat transfer rates of ternary nanofluid are increased by 11.2% compared to water.
- Ternary nanofluid attained maximum heat transfer rates compared to nanofluid and hybrid nanofluid.
- The entropy generation was minimized when CuO–MgO–TiO_2 nanoparticles were added into the base fluid.
- The magnetic field minimizes the entropy generation in ternary nanofluid.

Declaration of competing interest

The authors declare that they have no known competing financial interests or personal relationships that could have appeared to influence the work reported in this paper.

Acknowledgments

The authors would like to acknowledge the financial support from Universiti Teknologi Malaysia for the funding under UTM Fundamental Research (UTMFR: Q.J130000.3854.23H22).

References

[1] F. Shaikh, S.F. Shah, A. Siddiqui, L. Kumar, Application of recursive approach of pseudoplastic fluid flow between rotating coaxial cylinders, Alex. Eng. J. 61 (10) (2022) 7823–7832, http://dx.doi.org/10.1016/j.aej.2022.01.034.

[2] H. Laidoudi, H. Ameur, Investigation of the mixed convection of power-law fluids between two horizontal concentric cylinders: Effect of various operating conditions, Therm. Sci. Eng. Prog. 20 (2020) 100731, http://dx.doi.org/10.1016/j.tsep.2020.100731.

[3] S. Gouran, S. Mohsenian, S. Ghasemi, Theoretical analysis on MHD nanofluid flow between two concentric cylinders using efficient computational techniques, Alex. Eng. J. 61 (4) (2022) 3237–3248, http://dx.doi.org/10.1016/j.aej.2021.08.047.

[4] K. Abro, A. Abdon, A computational technique for thermal analysis in coaxial cylinder of one-dimensional flow of fractional Oldroyd–B nanofluid, Int. J. Ambient Energy 43 (1) (2022) 5357–5365, http://dx.doi.org/10.1080/01430750.2021.1939157.

[5] Y. Zhang, J. Jiang, Y. Bai, MHD flow and heat transfer analysis of fractional Oldroyd–B nanofluid between two coaxial cylinders, Comput. Math. Appl. 78 (10) (2019) 3408–3421, http://dx.doi.org/10.1016/j.camwa.2019.05.013.

[6] H. Hanif, S. Shafie, Impact of Al_2O_3 in electrically conducting mineral oil–based Maxwell nanofluid: Application to the petroleum industry, Fractal Fract. 6 (4) (2022) 180, http://dx.doi.org/10.3390/fractalfract6040180.

[7] A.K. Hamzat, M.I. Omisanya, A.Z. Sahin, O.R. Oyetunji, N.A. Olaitan, Application of nanofluid in solar energy harvesting devices: A comprehensive review, Energy Convers. Manage. 266 (2022) 115790, http://dx.doi.org/10.1016/j.enconman.2022.115790.
[8] H. Hanif, S. Shafie, Interaction of multi–walled carbon nanotubes in mineral oil based Maxwell nanofluid, Sci. Rep. 12 (1) (2022) 1–16, http://dx.doi.org/10.1038/s41598-022-07958-y.
[9] S.U. Choi, J.A. Eastman, Enhancing Thermal Conductivity of Fluids with Nanoparticles, Technical Report, Argonne National Lab.(ANL), Argonne, IL (United States), 1995, https://www.osti.gov/biblio/196525.
[10] H. Hanif, S. Shafie, Application of Cattaneo heat flux to Maxwell hybrid nanofluid model: a numerical approach, Eur. Phys. J. Plus 137 (8) (2022) 989, http://dx.doi.org/10.1140/epjp/s13360-022-03209-1.
[11] A.R. Amin, A. Ali, H.M. Ali, Application of nanofluids for machining processes: A comprehensive review, Nanomaterials 12 (23) (2022) 4214, http://dx.doi.org/10.3390/nano12234214.
[12] H. Hanif, S. Shafie, R. Roslan, A. Ali, Collision of hybrid nanomaterials in an upper–convected Maxwell nanofluid: a theoretical approach, J. King Saud Univ.-Sci. (2022) 102389, http://dx.doi.org/10.1016/j.jksus.2022.102389.
[13] M.S. Chavali, M.P. Nikolova, Metal oxide nanoparticles and their applications in nanotechnology, SN Appl. Sci. 1 (6) (2019) 607, http://dx.doi.org/10.1007/s42452-019-0592-3.
[14] S. Jafari, B. Mahyad, H. Hashemzadeh, S. Janfaza, T. Gholikhani, L. Tayebi, Biomedical applications of TiO_2 nanostructures: recent advances, Int. J. Nanomedicine (2020) 3447–3470, http://dx.doi.org/10.2147/IJN.S249441.
[15] S. Naz, A. Gul, M. Zia, R. Javed, Synthesis, biomedical applications, and toxicity of CuO nanoparticles, Appl. Microbiol. Biotechnol. 107 (4) (2023) 1039–1061, http://dx.doi.org/10.1007/s00253-023-12364-z.
[16] M. Chinthala, A. Balakrishnan, P. Venkataraman, V. Manaswini Gowtham, R.K. Polagani, Synthesis and applications of nano–MgO and composites for medicine, energy, and environmental remediation: a review, Environ. Chem. Lett. 19 (6) (2021) 4415–4454, http://dx.doi.org/10.1007/s10311-021-01299-4.
[17] H. Hanif, A finite difference method to analyze heat and mass transfer in kerosene based γ–oxide nanofluid for cooling applications, Phys. Scr. 96 (9) (2021) 095215, http://dx.doi.org/10.1088/1402-4896/ac098a.
[18] D. Naveena, R. Dhanabal, A.C. Bose, Investigating the effect of La doped CuO thin film as absorber material for solar cell application, Opt. Mater. 127 (2022) 112266, http://dx.doi.org/10.1016/j.optmat.2022.112266.
[19] T. Rymar, Use of water–TiO_2 nanofluid in horizontal Slinky collector of heat pump, Heat Transfer 2 (2022) 3, http://dx.doi.org/10.23939/jeecs2022.01.007.
[20] Y.B. Kho, R. Jusoh, M.Z. Salleh, M.H. Ariff, N. Zainuddin, Magnetohydrodynamics flow of Ag–TiO_2 hybrid nanofluid over a permeable wedge with thermal radiation and viscous dissipation, J. Magn. Magn. Mater. 565 (2023) 170284, http://dx.doi.org/10.1016/j.jmmm.2022.170284.
[21] A.D. Tuncer, A. Khanlari, A. Sözen, E.Y. Gürbüz, H.I. Variyenli, Upgrading the performance of shell and helically coiled heat exchangers with new flow path by using TiO_2/water and CuO–TiO_2/water nanofluids, Int. J. Therm. Sci. 183 (2023) 107831, http://dx.doi.org/10.1016/j.ijthermalsci.2022.107831.
[22] Y. Azmi, F. Ahmad, S. Kabir, Y. Lee, A. Zulfiqar, G. Yeoh, A. Qaiser, P.J. Masset, Investigating the mechanical performance of intumescent coating enhanced with magnesium oxide (MgO) for structural steel application, in: ICPER 2020: Proceedings of the 7th International Conference on Production, Energy and Reliability, Springer, 2022, pp. 927–938, http://dx.doi.org/10.1007/978-981-19-1939-8_69.
[23] İ. Aytaç, A.D. Tuncer, A. Khanlari, H.İ. Variyenli, S. Mantıcı, L. Güngör, S. Ünvar, Investigating the effects of using MgO–CuO/water hybrid nanofluid in an evacuated solar water collector: A comprehensive survey, Therm. Sci. Eng. Prog. (2023) 101688, http://dx.doi.org/10.1016/j.tsep.2023.101688.
[24] I. Tlili, H.A. Nabwey, S. Samrat, N. Sandeep, 3D MHD nonlinear radiative flow of CuO–MgO/methanol hybrid nanofluid beyond an irregular dimension surface with slip effect, Sci. Rep. 10 (1) (2020) 9181, http://dx.doi.org/10.1038/s41598-020-66102-w.
[25] W. Xiu, I. Animasaun, Q.M. Al-Mdallal, A.K. Alzahrani, T. Muhammad, Dynamics of ternary-hybrid nanofluids due to dual stretching on wedge surfaces when volume of nanoparticles is small and large: forced convection of water at different temperatures, Int. Commun. Heat Mass Transfer 137 (2022) 106241, http://dx.doi.org/10.1016/j.icheatmasstransfer.2022.106241.
[26] I.L. Animasaun, Q.M. Al-Mdallal, U. Khan, A.S. Alshomrani, Unsteady water–based ternary hybrid nanofluids on wedges by bioconvection and wall stretching velocity: Thermal analysis and scrutinization of small and larger magnitudes of the thermal conductivity of nanoparticles, Mathematics 10 (22) (2022) 4309, http://dx.doi.org/10.3390/math10224309.
[27] W. Cao, I. Animasaun, S.-J. Yook, V. Oladipupo, X. Ji, Simulation of the dynamics of colloidal mixture of water with various nanoparticles at different levels of partial slip: Ternary–hybrid nanofluid, Int. Commun. Heat Mass Transfer 135 (2022) 106069, http://dx.doi.org/10.1016/j.icheatmasstransfer.2022.106069.
[28] I.L. Animasaun, N.A. Shah, A. Wakif, B. Mahanthesh, R. Sivaraj, O.K. Koríko, Ratio of Momentum Diffusivity to Thermal Diffusivity: Introduction, Meta-Analysis, and Scrutinization, CRC Press, 2022, http://dx.doi.org/10.1201/9781003217374.
[29] S. Mousavi, F. Esmaeilzadeh, X. Wang, Effects of temperature and particles volume concentration on the thermophysical properties and the rheological behavior of CuO/MgO/TiO_2 aqueous ternary hybrid nanofluid: Experimental investigation, J. Therm. Anal. Calorim. 137 (2019) 879–901, http://dx.doi.org/10.1007/s10973-019-08006-0.
[30] R.R. Sahoo, V. Kumar, Development of a new correlation to determine the viscosity of ternary hybrid nanofluid, Int. Commun. Heat Mass Transfer 111 (2020) 104451, http://dx.doi.org/10.1016/j.icheatmasstransfer.2019.104451.
[31] A. Boroomandpour, D. Toghraie, M. Hashemian, A comprehensive experimental investigation of thermal conductivity of a ternary hybrid nanofluid containing MWCNTs–titania–zinc oxide/water–ethylene glycol (80: 20) as well as binary and mono nanofluids, Synth. Met. 268 (2020) 116501, http://dx.doi.org/10.1016/j.synthmet.2020.116501.
[32] N.K. Cakmak, Z. Said, L.S. Sundar, Z.M. Ali, A.K. Tiwari, Preparation, characterization, stability, and thermal conductivity of rGO–Fe_3O_4–TiO_2 hybrid nanofluid: An experimental study, Powder Technol. 372 (2020) 235–245, http://dx.doi.org/10.1016/j.powtec.2020.06.012.
[33] Z. Xuan, Y. Zhai, M. Ma, Y. Li, H. Wang, Thermo–economic performance and sensitivity analysis of ternary hybrid nanofluids, J. Mol. Liq. 323 (2021) 114889, http://dx.doi.org/10.1016/j.molliq.2020.114889.
[34] O. Mahian, A. Kianifar, C. Kleinstreuer, A.-N. Moh'd A, I. Pop, A.Z. Sahin, S. Wongwises, A review of entropy generation in nanofluid flow, Int. J. Heat Mass Transfer 65 (2013) 514–532, http://dx.doi.org/10.1016/j.ijheatmasstransfer.2013.06.010.
[35] P. Mondal, T. Mahapatra, MHD double–diffusive mixed convection and entropy generation of nanofluid in a trapezoidal cavity, Int. J. Mech. Sci. 208 (2021) 106665, http://dx.doi.org/10.1016/j.ijmecsci.2021.106665.
[36] H. Hanif, S. Shafie, N.A. Rawi, A.R.M. Kasim, Entropy analysis of magnetized ferrofluid over a vertical flat surface with variable heating, Alex. Eng. J. 65 (2023) 897–908, http://dx.doi.org/10.1016/j.aej.2022.09.052.
[37] N.K. Manna, N. Biswas, D.K. Mandal, U. Sarkar, H.F. Öztop, N. Abu-Hamdeh, Impacts of heater–cooler position and Lorentz force on heat transfer and entropy generation of hybrid nanofluid convection in quarter-circular cavity, Internat. J. Numer. Methods Heat Fluid Flow 33 (3) (2023) 1249–1286, http://dx.doi.org/10.1108/HFF-07-2022-0402.
[38] R.R. Sahoo, Thermo–hydraulic characteristics of radiator with various shape nanoparticle-based ternary hybrid nanofluid, Powder Technol. 370 (2020) 19–28, http://dx.doi.org/10.1016/j.powtec.2020.05.013.
[39] M. Bhatti, S.M. Sait, R. Ellahi, M.A. Sheremet, H. Oztop, Thermal analysis and entropy generation of magnetic Eyring–Powell nanofluid with viscous dissipation in a wavy asymmetric channel, Internat. J. Numer. Methods Heat Fluid Flow 33 (5) (2022) 1609–1636, http://dx.doi.org/10.1108/HFF-07-2022-0420.

[40] B. Mallick, J. Misra, Interplay of steric factor and high zeta potential on entropy generation during nanofluid slip flow in a microfluidic tube, Eur. Phys. J. Plus 137 (7) (2022) 868, http://dx.doi.org/10.1140/epjp/s13360-022-03069-9.

[41] R. Fares, F. Mebarek-Oudina, A. Aissa, S. Bilal, H.F. Öztop, Optimal entropy generation in Darcy–Forchheimer magnetized flow in a square enclosure filled with silver based water nanoliquid, J. Therm. Anal. Calorim. (2021) 1–11, http://dx.doi.org/10.1007/s10973-020-10518-z.

[42] H. Hanif, A. Khan, M. Rijal Illias, S. Shafie, Significance of Cu–Fe_3O_4 on fractional Maxwell fluid flow over a cone with Newtonian heating, J. Taibah Univ. Sci. 18 (1) (2024) 2285491, http://dx.doi.org/10.1080/16583655.2023.2285491.

[43] M. Shanmugapriya, R. Sundareswaran, P.S. Kumar, G. Rangasamy, Impact of nanoparticle shape in enhancing heat transfer of magnetized ternary hybrid nanofluid, Sustain. Energy Technol. Assess. 53 (2022) 102700, http://dx.doi.org/10.1016/j.seta.2022.102700.

[44] H. Hanif, Cattaneo–Friedrich and Crank–Nicolson analysis of upper-convected Maxwell fluid along a vertical plate, Chaos Solitons Fractals 153 (2021) 111463, http://dx.doi.org/10.1016/j.chaos.2021.111463.

[45] H. Hanif, A computational approach for boundary layer flow and heat transfer of fractional Maxwell fluid, Math. Comput. Simulation 191 (2022) 1–13, http://dx.doi.org/10.1016/j.matcom.2021.07.024.

[46] H. Hanif, S. Shafie, A. Chamkha, Effect of Ohmic heating on magnetohydrodynamic flow with variable pressure gradient: a computational approach, Waves Random Complex Media (2022) 1–16, http://dx.doi.org/10.1080/17455030.2022.2141916.